Nanoscale

Accepted Manuscript

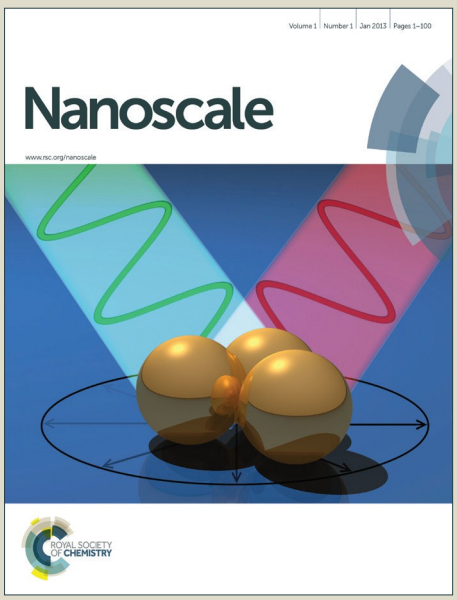

ROYAL SOCIETY OF CHEMISTRY

www.rsc.org/nanoscale

Journal Name

RSCPublishing

COMMUNICATION

Self-propelled Carbon Nanotube Based Microrockets for Rapid Capture and Isolation of Circulating Tumor Cells

Cite this: DOI: 10.1039/xoxxoooooox

Received ooth January 2012,
Accepted ooth January 2012

DOI: 10.1039/xoxxoooooox

www.rsc.org/

Shashwat S. Banerjee,[a] Archana Jalota-Badhwar,[c] Khushbu R. Zope,[b] Kiran J. Todkar,[a] Russel R. Mascarenhas, Govind P. Chate,[b] Ganesh V. Khutale,[a] Atul Bharde,[a] Marcelo Calderon[d] and Jayant J. Khandare[a,b]

Here, we report non-invasive strategy for isolating cancer cells by autonomously propelled carbon nanotube (CNT) microrockets. H_2O_2-driven oxygen (O_2) bubble-propelled microrockets were synthesized using CNT and Fe_3O_4 nanoparticles in the inner surface and covalently conjugating transferrin on the outer surface. Results show that self-propellant microrockets can specifically capture cancer cells.

Self-propelled micro-motors have paved the way to exciting applications in biomedical field such as delivering drugs, nanoscale transport and assembly, motion-based biosensing disease markers and microrobotics.[1-5] The usage of such micromachines to transport diverse payloads is one of the next prospects for nanomotor development.[6-8] Particularly chemically powered micro-/nanomotors based on different chemical compositions and structures, that are capable of moving autonomously in the presence of hydrogen peroxide fuel are being given emphasis.[4,5,9,10] Among these, self-propelled microshuttle is lucrative for practical biomedical applications.[4-9]. Especially, fabrication of nano and micropropellant systems featuring specific cell recognitions in shortest time frame is highly anticipated and yet challenging. Recently, ability of micromotors for selective capture, and isolation of cancer cells based on the selective binding and transport ability demonstrated.[6]

We report for the first time a chemically-powered CNT based magnetic micromachine for isolating and transporting cancer cells. Described microrocket technology could find a potential application as a bio-analytical micromachine for selective and rapid isolation of circulating cancer cells (CTCs). Detecting CTCs is a challenge due to the extremely low occurrence (10-100 per milliliter of blood) of CTCs among a large number of hematologic cells in the blood (10^9 mL^{-1}).[12,13] Several strategies, involving immunomagnetic beads or microfluidic devices, have been designed for isolating and accounting CTCs from blood.[14-16] However, most of these approaches are limited by their slow rate and low CTC-capture yield.[15,16] Currently, only one technology is available commercially (CellSearch®) to identify CTCs from the blood of cancer patients.[9]

We recently reported rapid and specific isolation of CTC based on magneto-dendritic nanosystem.[14] Here we show the preparation of bio-functionalized microrockets and their application for rapid isolation of cancer cells. Microrocket system consists of three functional components: (i) CNT, (ii) iron oxide (Fe_3O_4) nanoparticles for magnetic isolation, and (iii) Tf ligand (Tf) for specific targeting. Fe_3O_4 nanoparticles were loaded in the inner surface of CNTs as described previously with some modifications.[15] The unique advantages of the microrocket platform are: i) low density of microparticles ii) instantaneous propellant motion of microparticles (downward and upward) with an ability to '*strike*' cancer cells in its path, iii) rapid capture (~5 min) of TfR-overexpressing (TfR^+) cancer cells at the clinically relevant concentrations (approximately 1 CTC per 10^5 blood cells), iv) specific targeting ability due to presence of Tf ligand, which is generally used to capture cancer cells overexpressing TfR on their membranes, v) magnetic isolation of the captured cells owing to the presence of Fe_3O_4 nanoparticles and (v) large surface area and internal volume allows multiple components to be loaded onto the nanotube.

We followed a multi-step process (Figure 1A) to synthesize the Tf-CNT-Fe_3O_4 platform. Figure 1A displays the TEM image of Fe_3O_4-CNTs. We observed that Fe_3O_4 particles deposited inside CNT had a

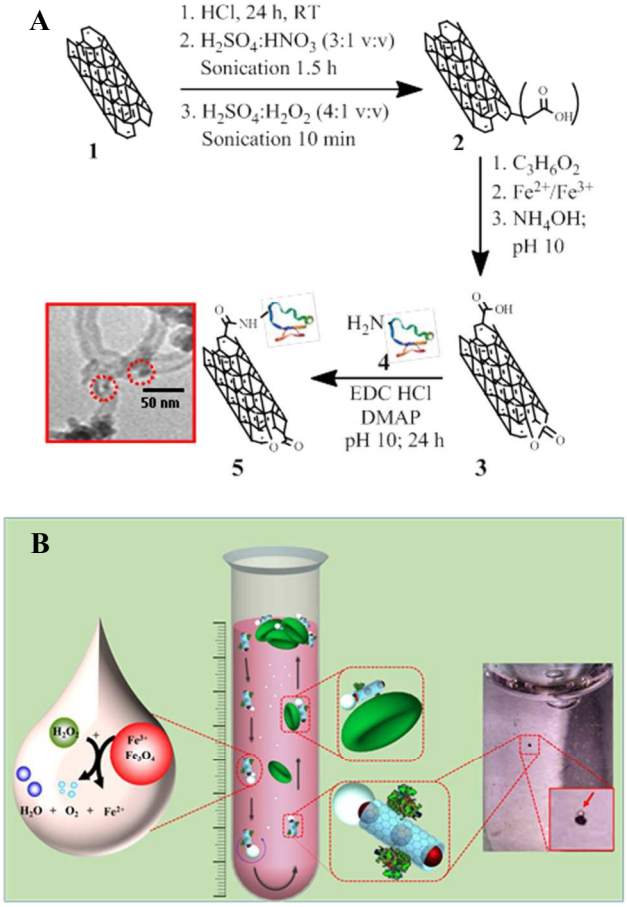

Figure 1. (A) Synthetic scheme for Tf-CNT-Fe_3O_4 showing the process steps. Inset shows a TEM image of Tf-Fe_3O_4-CNT. The presence of Fe_3O_4 in CNT is shown by red dotted circles. (B) Schematic of the driving mechanism for the Tf-Fe_3O_4-CNT microrocket. Right side inset shows the upward moving Tf-Fe_3O_4-CNT microrocket due to the adhered O_2 bubble indicated by an arrow.

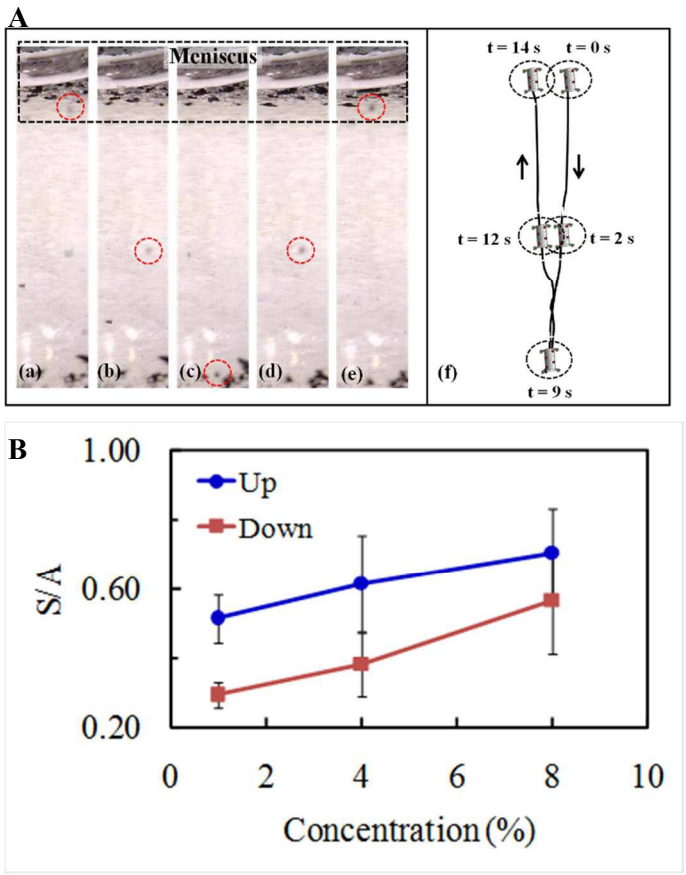

Figure 2. (A) Time-lapse images of a microrocket driven by oxygen bubble propulsion after time intervals of (a) 0, (b) 2, (c) 9, (d) 12 and (e) 14 s. (f) Motion trajectory of a typical Tf-Fe_3O_4-CNT microrocket in DMEM cell media containing 4% H_2O_2. Black dotted rectangle shows the Tf-Fe_3O_4-CNT microrocket floating at the meniscus. (B) Speed per unit area of Tf-CNT-Fe_3O_4microrockets in solutions of cell media with different H_2O_2 concentrations (1-8 w/w%) in downward and upward direction.

uniform size of ~ 6 nm (see supporting information; Figure S1). Moreover, the image indicates the successful assembly of the Fe_3O_4 nanoparticles in the nanotubes with 4~8 nm i.d. To further the confirm presence of Fe_3O_4 particles in CNT, Energy Dispersive X-ray fluorescence (EDXRF) profiling of Tf-CNT-Fe_3O_4 was demonstrated (see supporting information; Figure S2). The results clearly indicate the presence of Fe as a major element (99.2%) in Tf-CNT-Fe_3O_4 . Coupling of Tf on CNT-Fe_3O_4 composite was confirmed by Fourier transformed infrared (FTIR) spectroscopy (see supporting information; Figure S3). Further, Tf attachment quantified by a modified Bradford procedure was found to be ~ 0.2 mg of Tf per g of CNT-Fe_3O_4. The magnetic property of Tf-CNT-Fe_3O_4 particles was also visually evaluated in aqueous medium by placing it next to a permanent magnet (see supporting information; Figure S4).

Figure 1B illustrates the self-propulsion of suspended Tf-CNT-Fe_3O_4 microparticles mimicking microrocket in a solution containing H_2O_2. Microrockets initially propelled instantaneously towards the bottom of the tube and gradually reverted direction upwards. We noticed that the speed of the Tf-CNT-Fe_3O_4 microrocket was strongly dependent on the H_2O_2 concentration (see supporting information; Figure S5). As expected, the microrockets display highest speed at the maximum H_2O_2 (8%) concentration tested in aqueous solution. The upward directional speed of the microrockets decreases gradually from 0.90 mm•s^{-1} (at 8%) to 0.68 mm • s^{-1} (at 4%), and subsequently to 0.56 mm • s^{-1} (at 1%) per unit area of the particles. We hypothesize that microrocket motion is influenced by the surrounding H_2O_2 concentration as it affects the rate of the Fe^{3+} reduction to Fe^{2+}.

Notably such chemically powered micromotors are commonly incompatible with the high ionic strength environment of biological fluids and extending the scope of such microrockets to physiological conditions is a key challenge. So we studied the ability of our microrockets to propel in biological fluid such as Dulbaco's modified eagle medium (DMEM) cell media. Interestingly, the microrockets were found to propel efficiently even in DMEM containing 4% of H_2O_2. Figure 1B shows images of the microrocket at different vertical positions during its motion for a complete cycle. Initially, it was observed that microrockets, of smaller dimension, floated at the meniscus due to the low density and attached O_2 bubbles, formed by Fe_3O_4 nanoparticle catalyzed decomposition of H_2O_2. Once the smaller bubbles dispersed, a downward movement

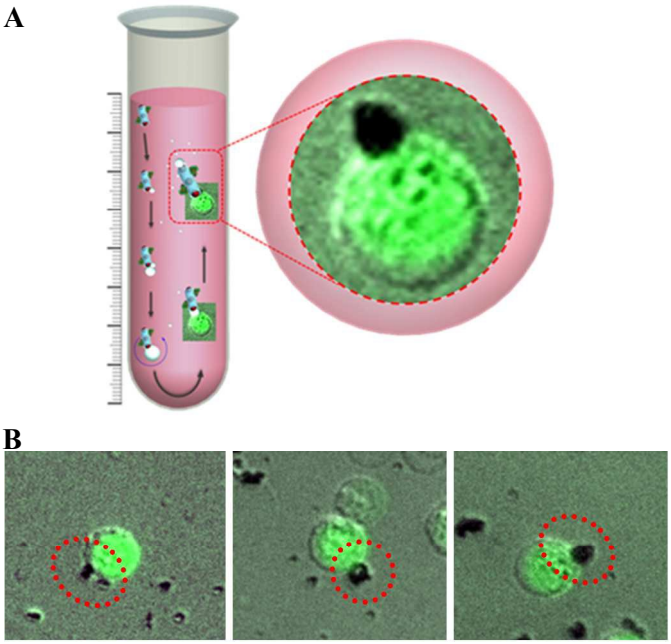

Figure 3. (A) CTC capture by microrocket. (B) Rapidity and specificity of the MDNS-cell interaction are confirmed by the images of Tf-CNT-Fe_3O_4 microrocket attached to the HCT116 cells in just 5 min.

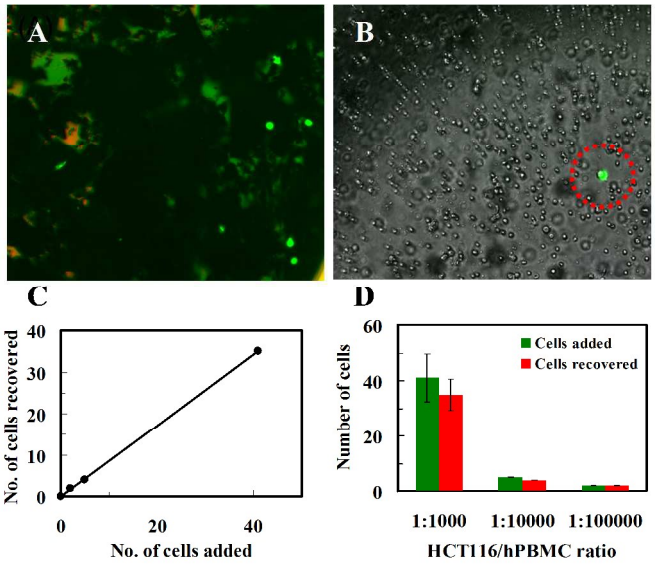

Figure 4. (A) Image of the magnetically isolated GFP-labelled HCT116 cells from an artificial CTC suspension (prepared in 1:10^3 HCT116: hPBMC ratio). GFP-labelled HCT116 cells can be seen to be attached to the black Tf-CNT-Fe_3O_4 particles. (B) Image of the remaining cell suspension after magnetic capture of the HCT116 cells. An HCT116 cell (shown by red arrow) is found to remain in solution. (C) Plot showing the number of recovered HCT116 cells from the artificial CTC suspension vs. the number of spiked cells. The capture efficiency from the slope of the regression line is estimated to be ~ 85%. (D) Plot showing cell capture (green: initial concentration; red: final concentration) by Tf-CNT-Fe_3O_4 microrocket from three different artificial CTC-like suspensions prepared in 1 x 10^3:1, 1 x 10^4 :1 and 1 x 10^5:1 (hPBMC:HCT116) ratios.

was observed (Figure 1B) due to the gravitational force. In the meantime, more O_2 bubbles formed and adhered to the Tf-CNT-Fe_3O_4 particle and in few seconds, the adhered O_2 bubble grew larger by coalescence of several smaller bubbles. Eventually the total volume of the bubble was sufficiently high, so that the buoyancy force balanced the gravitational and viscous forces and the microrocket moved upward (Figure 1B).[18,19] Figure 2A shows the tracking trajectory of a microrocket in cell media, indicating a vertical motion. It is noted that the microrocket moved with high average speed of 0.38 mm • s^{-1} in the downward direction and 0.62 mm • s^{-1} in the upward movement per unit area of the particle (about 12 and 16 times its body length per second). This corresponds to a large driving force of over 231 and 300 pN, based on the drag force $F=6\pi\mu rv$, where v is the speed, and μ is the viscosity of the medium and r is the radius of the microrocket. Further, when the concentration of H_2O_2 in cell media was varied there was notable effect on the speed as shown in Figure 2B. The speed of the microrocket at 8% H_2O_2 concentration was ~1.9 and~1.4 times higher in the downward and upward direction than at 1% of H_2O_2 concentration. Also, the number of times the microrocket moved up and down changed. At high H_2O_2 concentration (8%) the total distance moved by the microrocket was ~2 times more than that at lower concentration (1%) (see supporting information; Figure S6 and S7). Moreover, it was also revealed that the speed of the microrockets was only slightly affected in DMEM. The speed of the microrocket was 10% less in DMEM cell media compared to aqueous media containing 4% H_2O_2. Partial blocking of Fe_3O_4 surface by adsorbed proteins and increased solution viscosity may be responsible for this moderated speed.

We validated the application of microrockets for selective and rapid isolation of cancer cells from a heterogeneous population by separating HCT116 colon cancer cells from an artificial CTC suspension. We placed cell suspension in DMEM at the concentration of (1 x 10^6 cells mL^{-1}) containing 4% H_2O_2.

Tf-CNT-Fe_3O_4 microrockets were incubated in cell suspension for 5 min to target and isolate the HCT116 cells. We envisioned that Tf-functionalized microrockets could strike and selectively bind suspended HCT116 cells through the TfRs and finally transport them at the top of the tube from where they can be retrieved. Figure 3A illustrates the pick-up and transport of a cancer cell by a microrocket. On the other hand, Figure 3B shows cancer-cell-loaded microrocket. The force necessary for moving a relatively large (~16 μm) cancer cell is considerably high. The minimum force necessary for transporting such large cells at one body length per second in DMEM estimated from Stokes' law is 1.88 pN. The high speed of the microrocket is slightly affected by the cell loading (e.g., decreasing from 0.62 to 0.50 mm•s^{-1} in cell media), reflecting its high towing force.

We observed that Tf-CNT-Fe_3O_4 microrockets can efficiently pick-up and transport HCT116 cancer cells. We observed rapid action and selective targetability of Tf-CNT-Fe_3O_4 microrocket in capturing cells from a suspension. It also confirmed that the isolated cells remained normal for ~30 min and could be used for further studies (see supporting information; Figure S8). In addition, the HCT116 cell viability was also evaluated in DMEM containing 4% H_2O_2 after 1 hour. The study showed majority of the cells (78%) remained viable (see supporting information; Figure S8).

Furthermore, in order to confirm that the specific interaction of Tf-CNT-Fe_3O_4 microrocket with TfR^+ cells (such as, HCT116) is

because of Tf, we used CNT- Fe_3O_4 microrocket without Tf to capture TfR^+ cells (as a negative control). We found that no cells were attached to the CNT-Fe_3O_4 microrocket even after 5 min incubation. Hence, experiments with HCT116 confirm that after 5 min incubation, there is very little non-specific interaction of cells with the Tf-CNT-Fe_3O_4microrocket. In addition, to evaluate the effect of self propulsion of Tf-CNT-Fe_3O_4 microrocket on HCT116 capture, Tf-CNT (without Fe_3O_4) was used. It was found that Tf-CNT could capture only ~ 22% HCT116 cells (see supporting information; Figure S9). The study shows that self-propulsion of Tf-CNT-Fe_3O_4 microrocket plays a significant role in cell capture and isolation.

Our final goal was to quantify the capture efficiency of microrocket while targeting cancer cells from an artificial CTC suspension. We spiked human peripheral blood mononuclear (hPBMC) cells with TfR^+ GFP-labeled HCT116 cells in various hPBMC: HCT116 ratios (e.g. 1 x 10^3:1, 1 x 10^4:1 and 1 x 10^5:1). Cell suspensions of different ratios were incubated with Tf-CNT-Fe_3O_4 microrocket for 5 min prior to magnetic isolation. Following isolation, both the captured and the residual cell suspensions were imaged to estimate the number of captured and uncaptured HCT116-GFP cells in each sample. Assuming the number of captured HCT116-GFP cells to be N_C, the number of uncaptured HCT116-GFP cells to be N_U and following the method of Zheng *et al*, the capture efficiency (C.E.) for each dilution was estimated as:[20]

$$C.E. = N_C / (N_C + N_U) \quad (1)$$

Figure 4A shows image of captured cells (green) attached to the Tf-CNT-Fe_3O_4 particles (black). As expected, Tf-CNT-Fe_3O_4 particles are seen to aggregate following magnetic separation. Figure 4B shows an image of the residual cell suspension containing hPBMC cells and, in this particular case, a single uncaptured HCT116-GFP cell is seen (shown in red circle). Figure 4C shows a plot of recovered vs. spiked HCT116 cells. The % of recovered HCT116 cells for the clinically relevant range of HCT116:hPBMC ratios (1:1 x 10^4 to 1:1 x 10^5) are highlighted separately in the histogram of Figure 4D. Cell capture studies confirmed that Tf-CNT-Fe_3O_4 particles can successfully capture ~ 85% of the cancer cells within 5 min from a background of hPBMNCs even when the abundance of cancer cells is as low as ~0.001% of total number of cells.

Experimental Section

Preparation of CNT-Fe_3O_4 microparticle: Purification and oxidation of CNT were carried out using a previously described literature procedure.[20] Oxidized CNTs (AO-CNT) were then mixed with ethylene glycol and water. $FeCl_3 \cdot 6H_2O$ and $FeCl_2 \cdot 4H_2O$ were added to the mixture and sonicated for 2 h, followed by vigorous stirring for 4 h. The pH was adjusted to ~10 using NH_4OH. The resulting CNT-Fe_3O_4 microparticles were isolated by magnetic separation, washed with distilled water and dried overnight under vacuum.

Conjugation of Tf with CNT-Fe_3O_4: 2 mg of Tf was dissolved in 2 mL of D.I. water and 1.0 mg of the CNT-Fe_3O_4 was added to it. EDC.HCl was added to this reaction mixture (adding the same number of moles of EDC.HCl as Tf) and constantly stirred at room temperature for 4 h. The reaction time was limited to 4 h to avoid any possible intramolecular cross linking. Resulting Tf conjugated CNT-Fe_3O_4 microparticles were isolated by magnetic separation and dried at room temperature under vacuum.

Tf-CNT-Fe_3O_4-cell imaging: HCT116-GFP cells were plated at a density of 2 x 10^5 mL^{-1} on glass coverslips in 35 mm culture dishes. After 24 h, HCT116 cells in 1 mL DMEM were treated with 500 μg mL^{-1} of Tf-CNT-Fe_3O_4 in a NMR tube for 5 min and then subjected to magnetic field separation. The cell pellet obtained after a minute in the strong magnetic field was removed from the remaining cell suspension (containing uncaptured cancer cells). The captured cell pellet and the residual cell suspension was imaged by a Zeiss microscope (Zeiss, Observer.Z1) fitted with a 20 × objective using both bright field and fluorescence channels and the number of cells were counted using ImageJ plugin.[19]

Estimation of capture efficiency from artificial CTC suspension: Artificial CTC samples were prepared by spiking hPBMCs with GFP-labeled HCT116 cells at specific ratios (1:10^3-1:10^5 for HCT116:hPBMC respectively). 500 μg mL^{-1} Tf-CNT-Fe_3O_4 was added to the 1 mL of artificial CTC mixture incubated for 5 min and then subjected to magnetic field separation. The cell pellet obtained after a minute in the strong magnetic field was removed from the remaining cell suspension (containing hPBMCs and uncaptured cancer cells). The captured cell pellet and the residual cell suspension was imaged and the number of HCT116 cells were counted using ImageJ cell counter plugin.[21]

Motion parameters, cell culture, isolation of human hPBMC and characterization are included in the supporting information.

Conclusions

We demonstrated a novel CNT based microrocket that propels efficiently by the thrust of O_2 bubbles. The new self-propelled microrockets display ultrafast propulsion in aqueous solution as well as in DMEM. The microrocket displayed a driving force of over 231 and 300 pN in DMEM containing 4% H_2O_2. The speed and the distance travelled by the microrocket can be manipulated by changing the H_2O_2 concentration. The designed multifunctional microrocket has the ability to (i) rapidly target (~5 min) and efficiently capture (~85%) TfR^+ cancer cells from an artificial CTC-like suspension, (ii) magnetic isolation of the captured cells from peripheral blood cells and (iii) subsequent high resolution imaging. We envision that such self-powered micromotors may provide a new and unique approach for rapid and efficient extraction of CTCs from biological fluids and hence for the early diagnosis of cancer and its recurrence.

Notes and references

[a]Actorius Innovations and Research (AIR), 100 NCL Innovation Park, Pune-411008, India.
[b]Maharashtra Institute of Pharmacy, MIT Campus, Pune-411038, India.
[c]Cancer Biology Group, Piramal Life Sciences Ltd., Mumbai-400063, India.
[d]InstitutfürChemie und Biochemie, FreieUniversität Berlin, 14195 Berlin, Germany.

Electronic Supplementary Information (ESI) available: [details of any supplementary information available should be included here]. See DOI:10.1039/c000000x/

Acknowledgement

Authors thank Dr Preetam Ghogale for EDXRF analysis. Authors from Actorius Innovations and Research (AIR) wish to thank Dept. of Biotechnology, India for Biotech. Ignition Grant.

1 J. Wang, *ACS Nano,* 2009, **3**, 4.
2 W. Gao, R. Dong, S. Thamphiwatana, J. Li, W. Gao, L. Zhang, J. Wang, *ACS Nano,* 2015, 9, 117.
3 S. Sánchez, L. Soler, J. Katuri, Angew. Chem. Int. Ed. 2014, 53, 2.
4 D. A. Wilson, R. J. Nolte, J. C. van Hest, *Nat. Chem.,* 2012, **4**, 268.
5 M. G. van den Heuvel, C. Dekker, *Science,* 2007, **317**, 333.
6 S. Balasubramanian, D.el Kagan, C. J. Hu, S. Campuzano, M. J. Lobo-Castañon, N. Lim, D. Y. Kang, M. Zimmerman, L. Zhang, J. Wang, *Angew. Chem. Int. Ed.,* 2011*,* **50**, 4161.
7 S. Sundararajan, P. E.Lammert, A. W.Zudans, V. H.Crespi, A. Sen, *Nano.Lett.,*2008, **8**, 1271.
8 J. Burdick, R.Laocharoensuk, P. M. Wheat, J. D. Posner, J. Wang, *J. Am. Chem. Soc.,*2008, **130**, 8164.
9 L. Wang, K. Lee, Y. Sun, M. Lucking, Z. Chen, J. J. Zhao, S. B. Zhang *ACS Nano,*2009*,* **3**, 2995.
10 G. A. Ozin, I. Manners, S. Fournier-Bidoz, A. Arsenault, *Adv. Mater.,*2005, **17**, 3011.
11 K. Pantel, R. H. Brakenhoff, B. Brandt, *Nat. Rev. Cancer,*2008*,* **8**, 329.
12 J. Kaiser, *Science,*2010*,* **327**, 1074.
13 S. Wang, H. Wang, J. Jiao, K. J. Chen, G. E. Owens, K. Kamei, J. Sun, D. J. Sherman, C. P. Behrenbruch, H. Wu, H. R. Tseng,*Angew. Chem. Int. Ed.* 2009*,* **48**, 8970.
14 S. S. Banerjee, A. Jalota-Badhwar, S. D. Satavalekar, S. G. Bhansali, N. D. Aher, R. R. Mascarenhas, D. Paul, S. Sharma, J. J. Khandare, *Adv. Healthc. Mater.,* 2013*,* **2**, 800.
15 E. I. Galanzha, E. V. Shashkov, T. Kelly, J. W. Kim, L. Yang, V. P. Zharov, *Nat. Nanotechnol.,*2009*,* **4**, 855.
16 W. He, H. Wang, L. C. Hartmann, J. X. Cheng, P. S. Low, *Proc. Natl. Acad. Sci. U S A,*2007,**104**, 11760.
17 W. Chen, X. Pan, M. G.Willinger, D. S. Su, X. Bao, *J. Am. Chem. Soc.,* 2006*,* **128**, 3136.
18 S. K. Sailapu, A. Chattopadhyay, *Angew. Chem. Int. Ed.,*2014*,* **53**, 1521.
19 X. Zheng, L. S. Cheung, J. A. Schroeder, L. Jiang, Y. Zohar, *Lab Chip,*2011*,* **11**, 3269.
20 F. Forohar, C. Whitaker, W. M. Koppes. USA patent *US 7807127 B1* 2010.
21 Rasband, W.S., ImageJ, U. S. National Institutes of Health, Bethesda, Maryland, USA, http://imagej.nih.gov/ij/, 1997-2014.3